

Crystallography of Co/Cr bilayer magnetic thin films

K. Hono, B. Wong, and D. E. Laughlin

Department of Metallurgical Engineering and Materials Science and the Magnetic Materials Research Group, Carnegie Mellon University, Pittsburgh, Pennsylvania 15213

(Received 30 October 1989; accepted for publication 15 June 1990)

Various crystallographic textures of Co-alloy/Cr bilayer thin films are discussed based on microdiffraction and selected-area diffraction (SAD) results. In order to understand the origin of the crystallographic texture of the Co thin films, the orientation relationships between the Co and Cr grains were determined by the electron microdiffraction technique. From this information, we suggest that the $\{110\}$ Cr underlayer texture may not necessarily be required to obtain the highest in-plane coercivity in Co films. In order to evaluate the crystallographic texture of the film by SAD patterns, normalized intensity of SAD patterns for various thin-film textures have been calculated. Using these calculations, we interpret the SAD patterns taken from various Co and Cr thin films.

I. INTRODUCTION

Co alloy (Co implies Co and Co-based alloys like CoNi, CoNiCr, CoP, and so on) thin films deposited on Cr underlayers are the most promising candidates for high-density longitudinal recording media.¹ Since Lazzari, Melnick, and Randet^{2,3} discovered that a Cr underlayer increased the in-plane coercivity of Co thin films, many studies have been performed to understand this very important practical result.⁴⁻¹⁴ Recent papers on CoNi and CoNiCr alloy films deposited on Cr underlayers unanimously point to the importance of a $\{10\bar{1}1\}$ crystallographic texture as the cause of increased coercivity. This texture is believed to develop on a $\{011\}$ -textured Cr underlayer. Most of these conclusions were based on x-ray results which showed that the intensity of the $\{10\bar{1}1\}$ reflection increased when the Co alloy films were deposited on thick Cr underlayers which also showed intense $\{011\}$ x-ray reflections.^{8,11,12} Two transmission electron microscopic investigations^{13,14} support this conclusion based on electron diffraction patterns. However, the interpretation of the electron diffraction patterns was not complete, so that the results do not necessarily lead to the same conclusions which were derived from the x-ray investigations. Confusion seems to have arisen from the complexity of the reciprocal space with respect to the real space of the hcp crystals. For hcp crystals, the indices of the planes of real space do not necessarily correspond to the indices of the directions perpendicular to the planes and the reciprocal lattice planes. For example, a $[10\bar{1}1]$ zone axis does not imply that the $(10\bar{1}1)$ planes of Co are in the plane of the film.

The aim of this paper is to discuss the crystallographic texture in Co alloy thin films deposited on Cr underlayers (Co/Cr bilayer film) based on electron diffraction results. In order to understand the origin of the texture in Co films, the crystallographic orientation relationships (O.R.) between Co and Cr thin films have been determined by electron microdiffraction. We show herein that several low index planes of the bcc Cr underlayer can cause the c axis of the Co-based films to lie in the plane of the film. In the last part of this paper, a simple way to evaluate the crystallographic texture of both Co and Cr thin films by selected-area diffraction (SAD) patterns is presented.

II. ON THE $\{10\bar{1}1\}$ TEXTURE OF CO FILMS

It has been suggested that the $\{10\bar{1}1\}_{\text{Co}}$ texture is responsible for the high in-plane coercivity in CoNiCr/Cr thin films.^{8,11,12} As stated above, this is based on the fact that the intensity of the $\{10\bar{1}1\}$ x-ray reflection increases when Co films are sputtered on a Cr underlayer. Note, however, that in x-ray diffraction, the $\{10\bar{1}1\}$ reflection should be the most intense peak from a randomly oriented hcp polycrystal. According to the powder x-ray diffraction data,¹⁵ the intensity ratio $I_{(10\bar{1}0)}/I_{(10\bar{1}1)} = 0.2$ and $I_{(0002)}/I_{(10\bar{1}1)} = 0.6$. Hence, in order to conclude that the films are $\{10\bar{1}1\}$ textured, one has to show that the $\{10\bar{1}1\}$ intensity is significantly greater than five times that of the $\{10\bar{1}0\}$ peak. Since the $\{0002\}$ peak overlaps with the $\{011\}_{\text{Cr}}$ peak in a bilayer film, one cannot use the intensity ratio $I_{(10\bar{1}1)}/I_{(0002)}$ for evaluating the $\{10\bar{1}1\}$ texture. Although some papers^{8,11,12} concluded that the $\{10\bar{1}1\}$ texture of the CoNiCr films is the cause of the high coercivity, we could not find diffraction evidence in their results that clearly demonstrated that those films were indeed $\{10\bar{1}1\}$ textured. As stated before, even if the crystal orientation is random, the $\{10\bar{1}1\}$ peak should be five times higher than $\{10\bar{1}0\}$ peak. We did not find any x-ray patterns in the literature which showed convincingly that the intensity of $\{10\bar{1}1\}$ is more than five times greater than the $\{10\bar{1}0\}$ peak. Generally, the CoNiCr layer is in the range of tens of nanometers thick and the Cr underlayer is of the order of hundreds of nanometers; hence the x-ray diffraction intensity from Co layer is very weak compared to that from the Cr. Therefore, most of the x-ray peaks from Co cannot be distinguished from the background level (for example, see Fig. 2 of Ref. 12). When the deposited films are very thin, the x-ray diffraction patterns usually contain a great deal of background noise and sometimes even appear to be amorphous. The first peak which can be clearly detected should be the $\{10\bar{1}1\}$ peak, since its structure amplitude and multiplicity factor are both high. Hence, if the intensity of $\{10\bar{1}1\}$ peak is almost as weak as the background level as seen for example in Fig. 2 of Ref. 12, it is not likely that the rest of the peaks would appear with enough intensity to be distinguished from the background level. The conclusions drawn from such weak peaks are, therefore, not reliable. More definite evi-

dence of $\{10\bar{1}1\}$ texture and its correlation with the magnetic properties is needed, if we are to claim that the $\{10\bar{1}1\}$ texture enhances the coercivity of Co alloy thin films.

On the other hand, Ishikawa *et al.*¹⁰ demonstrated the Cr underlayer effect clearly by their x-ray diffraction pattern. The $\{10\bar{1}0\}_{Co}$ and $\{10\bar{1}1\}_{Co}$ peaks were clearly obtained from the CoNiCr sputtered on Cr underlayers, while only the $(0002)_{Co}$ peak was detected from CoNiCr film sputtered on glass substrate in their x-ray diffraction pattern. See Fig. 2 of Ref. 10. In this figure, the $(10\bar{1}0)$ peak is larger than the $(10\bar{1}1)$ peak; hence the intensity of the $(10\bar{1}0)$ plane is higher than that expected in randomly oriented polycrystal. In this sense, we can say this film was $\{10\bar{1}0\}$ textured, not $\{10\bar{1}1\}$ textured. From their figure, it is also obvious that CoNiCr sputtered on a glass substrate is strongly (0001) textured. Similar results will be shown by SAD patterns in the following section.

In addition to x-ray diffraction, selected-area electron diffraction (SAED or SAD) has been most commonly applied to evaluate the crystallographic texture of magnetic thin films. However, there seems to be some misunderstanding in interpreting the electron diffraction patterns in some of the literature.¹¹⁻¹⁴ For example, Lin, Alani, and Lambeth¹⁴ have indexed their SAD pattern from the Co film as $[01\bar{1}1]$ zone axis and concluded that $\{01\bar{1}1\}$ planes are dominant in the film plane. Note that the $[01\bar{1}1]$ direction is perpendicular to the irrational plane $(01\bar{1}1.756)$ assuming that the c/a ratio of the Co alloy is 1.623. The direction perpendicular to the $(01\bar{1}1)$ plane is the irrational direction, $[01\bar{1}0.569]$. In other words, finding the $[01\bar{1}1]$ zone axis pattern is not the same thing as having the $(01\bar{1}1)$ plane parallel to the surface. Indeed, the $[01\bar{1}1]$ direction is perpendicular to the irrational plane $(01\bar{1}1.756)$ which is 14.9° away from the $(01\bar{1}1)$. So the results by Lin *et al.* (14) do not prove that the $\{01\bar{1}1\}$ texture exists in the Co alloy thin film.

III. ELECTRON MICRODIFFRACTION

Electron microdiffraction [obtained from a small region (< 20 nm diameter) by a converged electron beam. It is different from convergent beam electron diffraction (CBED) in that the convergent angle is kept small by using a small condenser aperture so that higher angular resolution can be obtained.] is the most suitable technique to prove the existence of the $(10\bar{1}1)_{Co} \parallel (011)_{Cr}$ relationship between the Co and Cr grains. However, since the $(01\bar{1}1)$ planes do not have a rational zone axis or a rational reciprocal lattice plane, it does not seem easy to prove this commonly reported orientation relationship by electron diffraction. However, since one of the Laue conditions is relaxed in electron diffraction,¹⁶ there will be a good chance of observing a rational reciprocal lattice zone axis which is close to the irrational reciprocal lattice zone axis which is perpendicular to $(01\bar{1}1)$. As mentioned above, the zone axis perpendicular to the $(01\bar{1}1)$ plane is $[01\bar{1}0.569]$ assuming that $c/a = 1.623$ for Co alloy. The closest rational zone axis to this irrational zone is the $[02\bar{2}1]$, which is only 2.9° away from the $[01\bar{1}0.569]$. Hence, this zone axis diffraction pattern will appear if the $(01\bar{1}1)$ plane is perpendicular to the incident electron beam, i.e., if it lies in the plane of the film. Figure 1 shows an electron microdiffraction pattern from a Co-P/Cr bicrystal with a $[011]$ Cr zone axis.¹⁷ In this pattern, both the $[011]_{Cr}$ and $[20\bar{2}1]_{Co}$ patterns are superimposed. In addition to the fundamental spots from those two zone axes, many extra spots are observed. These extra spots can be accounted for by double diffraction due to the Co layer as schematically shown in Fig. 1(b). From this superimposed pattern, the following orientation relationship can be derived:

$$\begin{aligned} [011]_{Cr} &\parallel [20\bar{2}1]_{Co}, \\ (200)_{Cr} &\parallel (\bar{1}102)_{Co}. \end{aligned}$$

This relation was found whenever the Cr $[011]$ zone axis

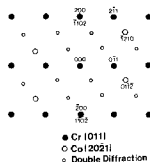
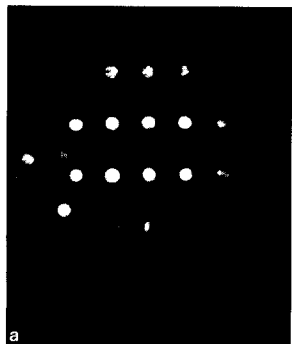


FIG. 1. (a) Electron microdiffraction pattern from Co-P/Cr bicrystal and (b) its schematic, showing the O.R. $[011]_{Cr} \parallel [20\bar{2}1]_{Co}, (200)_{Cr} \parallel (\bar{1}102)_{Co}$.

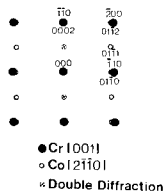
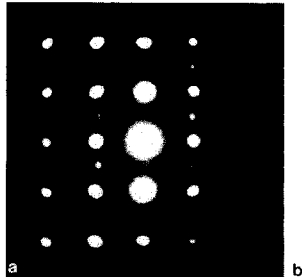


FIG. 2. (a) Electron microdiffraction pattern from CoNiCr/Cr bicrystal and (b) its schematic, showing the O.R. $[001]_{Cr} \parallel [2\bar{1}10]_{Co}$, $(\bar{1}\bar{1}0)_{Cr} \parallel (0002)_{Co}$.

was found in the underlayer. Thus we conclude that the $\{10\bar{1}\}$ Co planes are indeed grown on the $\{011\}$ Cr planes.

The diffraction pattern shown in Fig. 1 is similar to a $[011]$ bcc pattern containing $\{112\}$ twins.¹⁸ However, the possibility that this pattern could be due to bcc twins can be easily ruled out from the fact that this pattern was found only when Co films were deposited over the bcc Cr underlayer. Although many $\{011\}_{Cr}$ patterns were obtained from Cr films alone, no such "twinned" diffraction pattern was ever observed. Also, in the bright-field images of Cr films, no striation contrast indicating the existence of any planar faults was ever observed.

IV. ORIENTATION RELATIONSHIP

We have shown by microdiffraction that the $\{10\bar{1}\}$ plane is indeed grown on the $\{011\}$ Cr plane. In addition, we have found some other interesting orientation relationships (O.R.) from Co-alloy/Cr bilayer films. One of these microdiffraction patterns taken from a CoNiCr grain on top of a Cr grain is shown in Fig. 2. This CoNiCr film was sputtered on a strongly textured $\{001\}$ Cr underlayer. From Fig. 2, the following O.R. can be derived:

$$[001]_{Cr} \parallel [2\bar{1}10]_{Co},$$

$$(\bar{1}\bar{1}0)_{Cr} \parallel (0002)_{Co}.$$

This orientation relationship was previously observed from a Co/Cr bilayer by Daval and Randet.⁴ This orientation relationship is known as Pitsch-Schrader O.R., which is one of the most commonly observed O.R. in hcp/bcc systems.¹⁹ This microdiffraction pattern indicates that if a Cr grain of the underlayer has an $\{001\}$ plane surface in the film plane, the Co grain formed on it has its $\{2\bar{1}10\}$ plane in the film plane. Thus, the c axis can be kept in the plane on a $\{001\}$ Cr substrate. This should cause a higher in-plane anisotropy than the $\{10\bar{1}\}$ plane texture would.

More interestingly, the microdiffraction pattern from a $\{111\}$ Cr gave the following relationship¹⁷:

$$[\bar{1}11]_{Cr} \parallel [\bar{2}110]_{Co},$$

$$(110)_{Cr} \parallel (0002)_{Co}.$$

This O.R. is known as Burgers O.R.¹⁷ This microdiffraction pattern indicates that even if the underlayer Cr grain has a $\{111\}$ surface, the Co plane grown on it can have its $\{2\bar{1}10\}$ plane in the film plane. Hence the c axis will lie in the plane of the film.

The Burger's relation has also been observed when the underlayer Cr has either the $\{112\}$ or $\{113\}$ planes¹⁷ as follows:

$$[\bar{1}\bar{1}2]_{Cr} \parallel [0\bar{1}10]_{Co},$$

$$(110)_{Cr} \parallel (0002)_{Co}$$

and

$$[\bar{1}\bar{1}3]_{Cr} \parallel [\bar{1}010]_{Co},$$

$$(110)_{Cr} \parallel (0002)_{Co}.$$

This indicates that a $\{01\bar{1}0\}$ plane is grown on both the $\{112\}$ and $\{113\}$ underlayer Cr planes. Again, both of these O.R.'s have the c axis of the Co grain in the plane of the film.

From these findings, we can conclude that at least four major low-index planes of Cr (viz., $\{100\}$, $\{111\}$, $\{112\}$ and $\{113\}$) will cause the c axis of the Co layer to lie in plane, which will contribute to the high in-plane anisotropy. Either the $\{11\bar{2}0\}$ or $\{10\bar{1}0\}$ texture would cause a higher anisotropy field and may cause a higher in-plane coercivity than the $\{10\bar{1}\}$ texture. Since these four major low-index planes make the c axis in plane, the $\{011\}$ Cr texture may not be the one which optimizes the in-plane coercivity of Co alloy films.

From these O.R.'s identified on various plane surfaces, one sees that the O.R. is that which causes one of the directions in the Cr and Co interface to have the minimum strain, as shown in Fig. 3. In this figure, the $(defg)_{Co}$ plane is epitaxially grown on the $(hkl)_{Cr}$ plane. For example, on the $\{100\}$ and $\{111\}$ plane surface of Cr, the $\{\bar{1}\bar{1}20\}$ planes are grown so that the $(0002)_{Co}$ and $\{110\}$ planes are parallel.

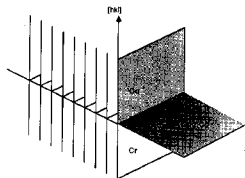


FIG. 3. Schematic illustration of the interface between Co and Cr grains, showing parallel planes at the interface. The zone axis is $[hkl]_{Cr}$.

On the $\{112\}$ and $\{113\}$ surface of Cr, $\{10\bar{1}0\}$ planes are grown so that the $(0002)_{Co}$ and $\{110\}_{Cr}$ planes are parallel. In such cases, the mismatch between the Cr and Co planes in the $[0001]$ direction is only 0.2%, since the interplanar spacing of $(0002)_{Co}$ is 2.035 Å and that of $(110)_{Cr}$ is 2.040 Å. As seen from the above examples, the orientation relationship between the two planes may be determined by a minimum strain criterion. However, in order to understand which Co plane will be grown on top of a certain Cr surface plane, we must consider the atomic matching as well. For example, although the $\{110\}_{Cr}$ plane would also allow the $(110)_{Co}$ and $(0002)_{Cr}$ to match up parallel to each other if either $\{\bar{1}120\}$ or $\{01\bar{1}0\}$ is grown on top of the $\{110\}_{Cr}$ surface, such an O.R. cannot be achieved since the two dimensional atomic matching is poor. As shown by Ohno *et al.*,¹¹ both the $\{10\bar{1}1\}_{Co}$ and $(0002)_{Co}$ planes have excellent atomic matching with the $\{011\}_{Cr}$ plane. So either of these planes could be grown on $\{011\}_{Cr}$ plane surface. Electron microdiffraction patterns showed the O.R.:

$$\begin{aligned} [011]_{Cr} &\parallel [20\bar{2}1]_{Co}, \\ (200)_{Cr} &\parallel (\bar{1}102)_{Co}. \end{aligned}$$

This implies that the $\{10\bar{1}1\}_{Cr}$ plane grew epitaxially on a $\{011\}_{Cr}$ plane. This O.R. can be shown to be equivalent to

$$\begin{aligned} [\bar{1}\bar{1}1]_{Cr} &\parallel [\bar{2}110]_{Co}, \\ (001)_{Cr} &\parallel (10\bar{1}1)_{Co}. \end{aligned}$$

In this case, the atomic matching in the $[\bar{1}\bar{1}1]$ direction of Cr is excellent ($\sim 0.28\%$), as both $[\bar{1}\bar{1}1]_{Cr}$ and $[\bar{2}110]_{Co}$ are close packed directions. In addition, the misfit strain in the direction orthogonal to $[\bar{1}\bar{1}1]_{Cr}$ (i.e., $[2\bar{1}1]_{Cr}$) is only $\sim 2.1\%$. The atomic density on the $(10\bar{1}1)_{Co}$ plane is 0.173 \AA^{-2} , which is very close to the atomic density of $(011)_{Cr}$ (~ 0.170). On the other hand, if the $(0001)_{Co}$ plane is epitaxially grown on a $\{011\}_{Cr}$ with the Burgers O.R., the misfit strain in the $[2\bar{1}1]_{Cr}$ is 7.8%. Also, the atomic density of the $(0002)_{Co}$ plane is 0.184 \AA^{-2} , significantly larger than that of $(011)_{Cr}$. From these calculations, we speculate that the $\{10\bar{1}1\}_{Cr}$ planes cause less interfacial strain than the $(0002)_{Co}$ basal planes when grown epitaxially on $(001)_{Cr}$. Of course, if the c/a ratio of the Co alloy is much different from 1.623, different results may occur.

V. TEXTURE EVALUATION BY SELECTED-AREA DIFFRACTION PATTERN

The texture of Co-based films that are deposited onto glass substrates can be readily measured by x-ray diffraction. However, the texture of Co films that are on hard disks can not be easily measured, because of the various diffraction peaks present in addition to the hcp Co ones. These include peaks from the bcc Cr underlayer, the fcc Al-based alloy substrate, and the broad amorphous peak of the electroplated Ni-P film. Therefore, it is useful to present a qualitative way of studying the texture of Co-based films deposited on hard disks, namely by means of selected-area (electron) diffraction (SAD).

First, a brief summary of the geometry and the crystallography of thin films is appropriate. Figure 4 shows a schematic of a thin film that has the (hkl) planes in the film plane. The vertical line is the zone axis of the film. For this film, using x-ray diffraction, only the (hkl) reflections will appear. On the other hand, if this film were placed in an electron microscope and the beam were almost parallel to the zone axis, only those planes of the zone $[uvw]$ would diffract, viz., those planes with their normals $\sim 90^\circ$ to the zone axis. For example, a film with (0001) planes of the hcp structure will give rise to a strong (0002) x-ray reflection, but not to any (0002) electron diffraction spots. To get a (0002) reflection by electron diffraction, the c axis must be in the plane of the film. Of course, x-ray diffraction would not detect the (0002) planes in this case. Note again that $[hkl]$ zone axis is not perpendicular to (hkl) plane if l is not zero in the case of the hcp structure.

When the thin film is strongly textured, it is easy to tell the texture not only by selected-area diffraction patterns, but also by electron microdiffraction patterns.¹³ However, if the amount of the texture is not strong, it is usually not possible to determine the texture by taking microdiffraction patterns from individual grains, because the small number of patterns that can be observed lack statistical significance. Also, if the crystals are randomly oriented, the occurrence of some specific zone axis pattern would be proportional to its multiplicity factor; hence, the occurrence of (0001) would be less than other planes even if the crystals are randomly oriented, since the multiplicity factor of (0001) is only two. Therefore, unless a large majority of the patterns taken by microdiffraction show some specific zone axis pattern, it is generally very difficult to evaluate the texture by microdiffraction.

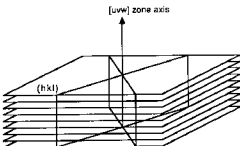


FIG. 4. Schematic illustration of the geometry of (hkl) planes and $[uvw]$ zone axis.

TABLE I. Calculated normalized intensity of SAD ring patterns from random and textured polycrystal samples of Co.

<i>hkl</i>	Random	[0001]	[11 $\bar{2}$ 0]	[10 $\bar{1}$ 0]	[20 $\bar{2}$ 1]
10 $\bar{1}$ 0	27	100	27	0	0
0002	27	0	80	100	0
10 $\bar{1}$ 1	100	0	100	0	0
10 $\bar{1}$ 2	11	0	11	0	91
1 $\bar{1}$ 20	12	46	0	15	100
10 $\bar{1}$ 3	13	0	13	0	0
20 $\bar{2}$ 0	2	6	2	0	0
1 $\bar{1}$ 22	13	0	0	16	0
20 $\bar{2}$ 1	9	0	9	0	0
0004	2	0	5	6	0

We can, however, study the texture of films by SAD. In this case, the number of grains included in the intermediate aperture is sufficient to give qualitative significance to the observed texture. In order to evaluate the texture of the Co and Cr thin films qualitatively by SAD patterns, the intensity ratio for the SAD rings was calculated based on the following equation of Vainshtein²⁰:

$$I_{hkl} = J_0 \lambda^2 \left(\frac{\Phi_{hkl}}{\Omega} \right)^2 \Delta V \frac{d_{hkl}^2 p}{4\pi L \lambda},$$

where I_{hkl} is the local intensity of a (*hkl*) diffraction ring, J_0 is the intensity of the incident electron beam, λ is wavelength of the electrons, Φ_{hkl} is the structure amplitude, Ω is the volume of the unit cell, ΔV is the volume of the crystal, p is the multiplicity factor for the *hkl* planes, and L is the distance between the specimen and the film. This equation shows that the local integrated intensity of the diffraction ring is proportional to the product of the square of the structure amplitude, the square of the d spacing, and the multiplicity factor, or

$$I_{hkl} = k |\Phi_{hkl}|^2 d_{hkl}^2 p,$$

where k is a constant within a single diffraction pattern. Based on this equation, the intensity ratio of each diffraction ring for various textures can be easily calculated. The results are as shown in Tables I and II for the Co films and Cr films, respectively.

When the crystal is randomly oriented, the normalized intensity of the diffraction rings are similar to those of the powder x-ray diffraction pattern. (They are not exactly the same, since the atomic scattering factors for electrons and

TABLE II. Calculated normalized intensity of SAD ring patterns from random and textured polycrystal samples of Cr.

<i>hkl</i>	Random	[011]	[001]	[111]	[012]
110	100	100	100	100	0
200	13	26	25	0	100
211	22	22	0	11	85
220	5	6	6	5	0
310	6	0	6	0	0
222	1	4	0	0	0
321	6	0	0	3	11
400	0.2	1	0.9	0	4

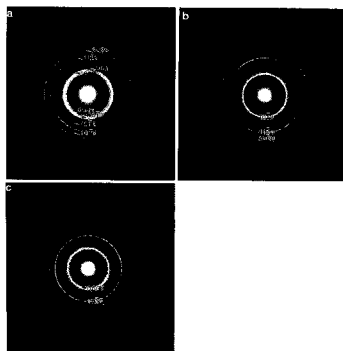


FIG. 5. SAD patterns from (a) CoNiCr film deposited on Cr underlayer, (b) CoNiCr film deposited on glass substrate, and (c) CoNiCr very thin film deposited on glass substrate, showing various crystallographic textures.

rays depend differently on $\lambda/\sin \theta$. Also the Lorentz-polarization factor is omitted in the case of electron diffraction, since θ is small.) When some texture exists, the normalized intensity changes significantly and some diffraction rings may disappear. Here the texture is assumed to be a "fibrous texture"; that is, one which has a particular crystal axis aligned along a certain direction, with a random arrangement of azimuthal orientations about this axis.²¹ For the case of a thin film, the "fibrous axis" is just the normal to the film. For such a textured film, the intensity was calculated by changing the multiplicity factor which can be easily found from the number of poles on the great circle at 90° to the normal to the film plane. Note that the incident electron must be parallel to the zone axis of the texture (normal to the film plane) to compare the results with these tables. If the in-plane orientation is also textured, the rings would break up into arcs, centered on the spot pattern of the corresponding reciprocal plane. If the incident electron is tilted from the normal to the thin film, the rings will produce some local reflections inside the ring, and as a result, the entire pattern will look ellipsoidal (see Refs. 20 and 21). In such a case, the sample should be carefully tilted to detect the texture.

Some examples of SAD patterns are shown in Fig. 5. Figure 5(a) is a typical SAD pattern from CoNiCr film which was deposited on Cr underlayer. The first three rings, corresponding to the {10 $\bar{1}$ 0}, {0002}, and {10 $\bar{1}$ 1} rings, respectively, are observed with almost equal intensity, although the first ring is slightly weaker. The fourth broad weak ring just outside the {10 $\bar{1}$ 1} is from the {002} fcc Co.²² The intensity ratio of the first three rings does not follow the calculated intensity of randomly oriented grains. If grains were randomly oriented, the second ring, the {0002}, should

be significantly weaker than the third ring, the $\{10\bar{1}\}$. If this film is $\{11\bar{2}\}$ textured, the intensity of the (0002) ring would be closer to that of $\{10\bar{1}\}$. However, we can clearly observe the $\{11\bar{2}\}$ ring which is not expected from a $\{11\bar{2}\}$ texture. If we assume that $\{11\bar{2}\}$ and $\{10\bar{1}\}$ planes are predominant in this film plane, the (0002) intensity would be higher than expected from $\{11\bar{2}\}$ texture, and in addition, a $\{11\bar{2}\}$ ring should also be present. Hence, we can speculate from this SAD pattern that both the $\{11\bar{2}\}$ and $\{10\bar{1}\}$ planes are more abundant than other planes. This means that the c axes of the Co grains would mainly lie in the plane of the film. As seen from this example, it is not easy to evaluate the degree of texture from the SAD patterns if the films are not strongly textured.

It is well known that Co grains develop strong (0001) texture when they are deposited on glass substrates. Figure 5(b) is a typical SAD pattern from CoNiCr deposited on a glass substrate. The $\{10\bar{1}\}$, $\{11\bar{2}\}$, and $\{20\bar{2}\}$ rings are clearly observed, while (0002) , $\{10\bar{1}\}$, and $\{10\bar{1}\bar{2}\}$ rings are not present. Comparing the intensity ratio with Table I, we conclude that this film is strongly (0001) textured. Note that by the overlapping of some fcc rings, some additional rings are observed (for example, the ring at the $\{11\bar{2}\}$ position just outside the $\{20\bar{2}\}$ ring is due to a $\{311\}$ fcc ring). If the grains are strongly textured like this, there is no difficulty in ascertaining this from the SAD patterns.

One interesting example from CoNiCr film deposited on glass substrate is shown in Fig. 5(c). This film is formed by very short sputtering period and estimated to be less than 5 nm thick. The (0002) ring is noticeably stronger than any other rings, and the $\{11\bar{2}\}$ and $\{20\bar{2}\}$ rings have a fair intensity. This suggests that this film is $\{10\bar{1}\}$ textured. As shown above, the thick CoNiCr film deposited on glass has strong (0001) texture. However, this texture was not found to be present from the very early stage of deposition. This indicates that the texture of Co films grown on glass is not governed by the nucleation of some preferential direction, but that it is developed by the preferential growth of the grains with $[0001]$ directions. A similar result in the case of Cr is shown below.

Some examples of SAD patterns from Cr thin films are shown in Fig. 6. Figures 6(a) and 6(b) are both taken from the same film, but from different thicknesses. Figure 6(a) was taken from the top region of a film approximately 400 nm thick, and Fig. 6(b) is taken from the bottom region of the same film (substrate side). These SAD patterns show a large difference, even though both are taken from the same film. The intensity of the SAD pattern from the bottom of the film [Fig. 6(b)] follows closely the calculated values for randomly oriented grains. On the other hand, the SAD pattern from the top part of the film [Fig. 6(a)] indicates that this region is textured, since the intensity ratio is quite different from that expected from the randomly oriented film. The intensity of the $\{011\}$ ring is weaker than $\{002\}$ and $\{11\bar{2}\}$ rings. Also the $\{002\}$ and the $\{11\bar{2}\}$ rings have almost equal intensity. This result is puzzling, since x-ray diffraction showed only a single strong $\{011\}$ peak. However, again $\{011\}$ is always detected as the strongest peak in x-ray diffraction, so if the film thickness is not large enough, other

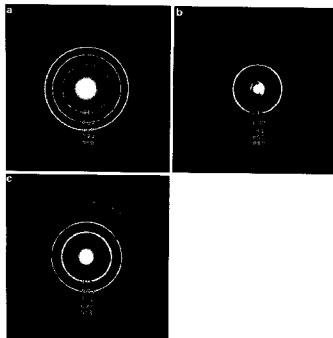


FIG. 6. SAD patterns of (a) top region and (b) bottom region of 400-nm Cr film deposited on glass substrate, showing that the texture varies as the film grows. (c) A typical SAD pattern of (001) textured Cr.

weak peaks may be smeared out by the background. Actually, the microdiffraction showed various zone axis patterns. Again, since this film is not strongly textured, it is not easy to specify its texture from the SAD pattern alone. From the fact that $\{002\}$ and $\{11\bar{2}\}$ have almost equal intensity, the occurrence of the (012) zone axis may be higher than random distribution. In addition, the (011) zone may also be more abundant than in a random configuration. The existence of (011) will contribute $\{011\}$ intensity, but it will not change the intensity ratio of $\{002\}$ and $\{11\bar{2}\}$ diffraction rings. Since the SAD pattern from the bottom part showed that the crystal orientation was random in the initial deposition stage, we can conclude that the texture in the Cr films was developed by the preferential growth of the grains with some specific direction.

A final example from a Cr film is shown in Fig. 6(c). This pattern corresponds closely with the calculated intensity ratio for $\{001\}$ texture. The $\{11\bar{2}\}$ ring, which is usually very strong, is essentially absent. Most of the microdiffraction patterns taken from this film were (001) zone axis patterns.

V. CONCLUSION

In this paper we have discussed various issues involved with the crystallographic texture of Co/Cr bilayer thin films. We have shown by TEM that in some cases the $\{10\bar{1}\}_{Co}$ planes lie in the plane of the film parallel to the $\{011\}_{Cr}$ planes. We have also shown that other planes of Co can lie in the film plane. For example, $\{10\bar{1}\}_{Co}$ has been shown to lie in the plane of the film parallel to $\{11\bar{2}\}_{Cr}$, and $\{11\bar{2}\}_{Co}$ and $\{11\bar{2}\}_{Co}$ planes lie in the plane of the film

parallel to $\{111\}_{Cr}$ and $\{100\}_{Cr}$. Thus we believe that by careful manipulation of the Cr underlayer texture, the in-plane anisotropy of Co-based alloy films can be enhanced. For this purpose, the $\{011\}_{Cr}$ underlayer texture may not be the best one. Finally, in the last section of the paper a simple, qualitative method of evaluating the crystallographic texture of Co and Cr thin films by SAD patterns was presented. Although quantitative information on the texture of films cannot easily be obtained by SAD patterns, the method is helpful in the study of layered films since the underlayers are thinned away before observation.

ACKNOWLEDGMENTS

This work was jointly supported by the Magnetic Technology Center and the Magnetic Materials Research Group at Carnegie Mellon University (DMR-86-13386). Some of the samples used in this study were prepared by S.-L. Duan of CMU.

¹J. K. Howard, *J. Vac. Sci. Technol.* **A 4**, 1 (1986).

²J. P. Lazzari, I. Melnick, and D. Randet, *IEEE Trans. Magn.* **MAG-3**, 205 (1967).

³J. P. Lazzari, I. Melnick, and D. Randet, *IEEE Trans. Magn.* **MAG-5**, 955 (1969).

⁴J. Daval and D. Randet, *IEEE Trans. Magn.* **MAG-6**, 768 (1970).

⁵H. J. Lee, *J. Appl. Phys.* **57**, 4037 (1985).

⁶T. Yamada, N. Tani, M. Ishikawa, T. Ota, K. Nakamura, and A. Itoh, *IEEE Trans. Magn.* **MAG-21**, 1429 (1985).

⁷T. Abe and T. Nishihara, *IEEE Trans. Magn.* **MAG-22**, 570 (1986).

⁸G.-L. Chen, *IEEE Trans. Magn.* **MAG-22**, 334 (1986).

⁹H. Yamaguchi and M. Yanagisawa, *IEEE Trans. Magn.* **MAG-22**, 576 (1986).

¹⁰M. Ishikawa, N. Tani, T. Yamada, Y. Ota, K. Nakamura, and A. Itoh, *IEEE Trans. Magn.* **MAG-22**, 573 (1986).

¹¹T. Ohno, Y. Shirotshi, S. Hishiyama, H. Suzuki, and Y. Matsuda, *IEEE Trans. Magn.* **MAG-23**, 2809 (1989).

¹²H. J. Lee, *J. Appl. Phys.* **63**, 3269 (1988).

¹³J.-W. Lee, K. R. Mountfield, and D. E. Laughlin, *J. Appl. Phys.* **63**, 3266 (1988).

¹⁴T. Lin, R. Alani, and D. N. Lambeth, *J. Magn. Magn. Mater.* **78**, 213 (1989).

¹⁵JCPDS diffraction data card, JCPDS, 1601 Park Lane, Swarthmore, Pennsylvania.

¹⁶J. W. Edington, *Practical Electron Microscopy in Materials Science, 2. Electron Diffraction in the Electron Microscope* (Philips, Eindhoven, 1975).

¹⁷K. Hono and D. E. Laughlin (unpublished).

¹⁸C. M. Wayman and R. Bullough, *Trans. Met. Soc. AIME* **236**, 1711 (1966).

¹⁹U. Dahmen, *Acta Metall.* **30**, 63 (1982).

²⁰B. K. Vainshtein, *Structure Analysis by Electron Diffraction* (MacMillan, New York, 1964).

²¹P. Hirsch, A. Howie, R. B. Nicholson, D. W. Pashley, and M. J. Whelan, *Electron Microscopy of Thin Crystals* (Butterworths, London, 1967), p. 116.

²²K. Hono, B. G. Demczyk, and D. E. Laughlin, *Appl. Phys. Lett.* **55**, 229 (1989).